https://doi.org/10.5194/egusphere-2024-2451
Preprint. Discussion started: 7 August 2024

Anthropogenic pressures driving the salinity intrusion in the Guadalquivir Estuary: Insights from 1D Numerical Simulations

Sara Sirviente[1], Juan J. Gomiz-Pascual[1], Marina Bolado-Penagos[1], Sabine Sauvage[2], José M. Sánchez-Pérez[2], Miguel Bruno[1].

[1]Department of Applied Physics, Faculty of Marine and Environmental Sciences, Marine Research Institute (INMAR), International Campus of Excellence of the Sea (CEI·MAR), University of Cadiz, Puerto Real, 11510 Cadiz, Spain
[2]Centre de Recherche sur la Biodiversité et l'Environnement (CRBE), Université de Toulouse, CNRS, IRD, Toulouse INP, Université Toulouse 3 – Paul Sabatier (UT3), Toulouse, France

Correspondence to: Sara Sirviente (sara.sirviente@uca.es)

Abstract. The study presents a dynamic analysis of the present day behavior of saline intrusion in the Guadalquivir estuary and evaluates the impact of anthropogenic pressures on the dynamics of the salt wedge. A one-dimensional (1D) hydrodynamic model with a transport and dispersion module is used to study the effects of human pressure involved in the salinity concentration along the estuary. The observations, which correspond to continuous measurements taken during different oceanographic campaigns from 2021 to 2023, show an excessive penetration of the salt wedge in the estuary (with salinities of 5 psu at km 60) as compared to the idealized situation when anthropogenic water withdrawals are absent. This highlights the need to include a water withdrawal term in the simulations to accurately reproduce the real behavior of the system. Thus, reflecting the magnitude of the anthropogenic pressures. The model successfully reproduces the observations when this forcing factor is included. Under constant low flow conditions, experiments show that increasing water withdrawals leads to an increase in upstream saline intrusion. Similarly, under constant water withdrawal conditions, a decrease in saline intrusion is observed when freshwater flows exceed 40 m^3/s. Variations in anthropogenic pressures, such as water withdrawals for agriculture or industry and reductions in freshwater flow, play a fundamental role in the evolution of saline intrusion. Under the current circumstances, the Guadalquivir estuary requires an urgent regulation of these uses in order to avoid further damage on the aquatic ecosystems.

1.Introduction

Estuaries are considered one of the most valuable and threatened ecosystems in the world (Lopes et al., 2024). Under optimal conditions, estuary mouths are biologically more productive than rivers and adjacent ocean zones because of the high concentration of nutrients that stimulates higher primary productivity (Miranda et al., 2017). The characteristics of estuarine communities are strongly and directly linked to physical parameters, such as temperature, turbidity, and salinity (Dauvin, 2008). These coastal regions play a key role in supporting significant socioeconomic and environmental activities, serving as essential nursery habitats on continental shelves and providing invaluable ecosystem services to other ecological systems

https://doi.org/10.5194/egusphere-2024-2451
Preprint. Discussion started: 7 August 2024

(Donázar-Aramendía et al., 2019). However, estuaries have been severely degraded by anthropogenic activities. In recent decades, land use for agriculture and changes in channel geomorphology for navigation and other purposes have altered the natural hydrodynamics, morphology, and water quality conditions of these systems (Sirviente et al., 2023; Gomiz-Pascual et al., 2021). Water abstraction for activities such as irrigation, domestic use, and industrial activities is the most significant factor contributing to the degradation of these ecosystems (Algaba et al., 2024)

The Guadalquivir River Estuary (GRE) (Fig. 1) is a positive and well-mixed estuary (Pritchard,1952; Losada et al., 2017), although it deviates from this definition during periods of heavy flooding (Álvarez et al., 2001). It is a meso-tidal estuary with semi-diurnal tidal components being the most energetic (Reyes-Merlo et al., 2013). Saltwater intrusion is fundamentally linked to these tidal dynamics, which vary in amplitude in cycles of spring and neap tides of approximately 14.5 days (Contreras and Polo, 2012). Flowing into the Atlantic Ocean, this estuary is one of the most important socioeconomic areas in southern Spain. It extends 110 km from its mouth in Bonanza to its head at the Alcalá del Río dam (Fig. 1a), with the first 85 km being navigable, making it the only navigable river in Spain (Navarro et al., 2011).

The dam (black triangle in Fig. 1) strongly regulates freshwater input to the estuary by blocking upstream tidal waves (Contreras and Polo, 2012), creating a closed boundary in this semi-enclosed channel, and causing the tidal wave to arrive with sufficient energy to reflect and interact with the incident wave (Diez-Minguito et al., 2012). The largest freshwater input (80%) to the estuary is through the dam, the last point in the extensive network of reservoirs that regulate the GRE basin. This estuary is characterized by low-flow conditions (< 40 m3/s) most of the time (75% of the year), where tidal dominance and well-mixed conditions prevail (Siles-Ajamil et al., 2019). In contrast, during high-flow conditions (> 400 m3/s), tidal propagation is disrupted, increasing the potential energy of the water column and decreasing upstream saline water intrusion (Diez-Minguito et al., 2013; Ruiz et al., 2015).

https://doi.org/10.5194/egusphere-2024-2451
Preprint. Discussion started: 7 August 2024

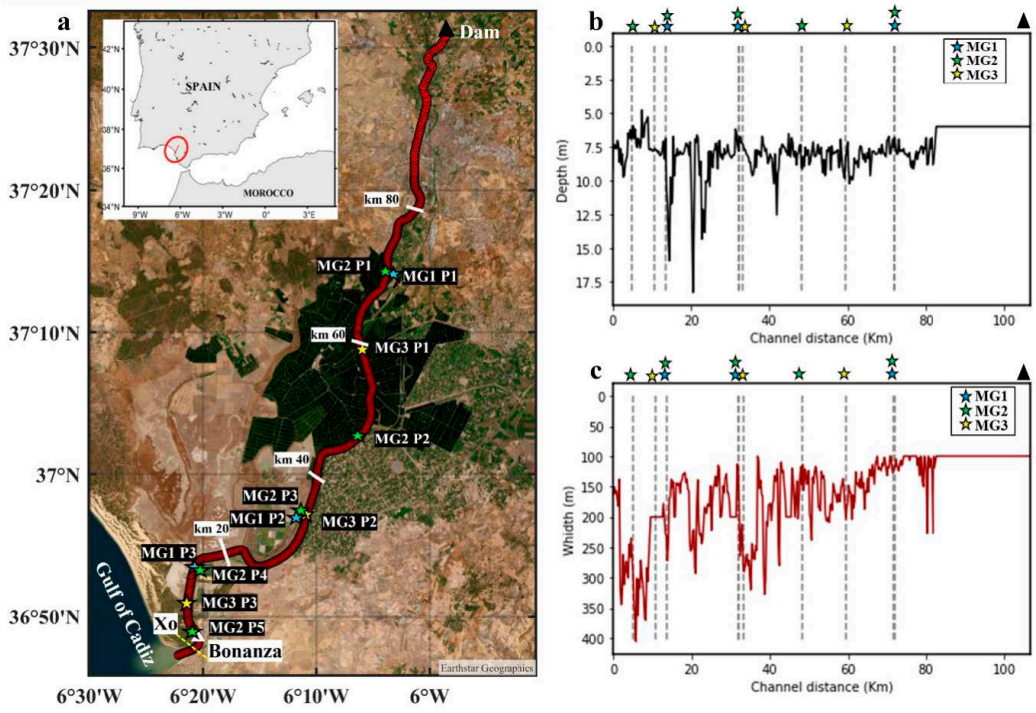

Figure 1: (a) Geographic region of the study area. Xo represents the starting section of the simulations; the white triangle indicates Bonanza point. The blue, green and yellow stars represent the sample points for each campaign MG1, MG2, and MG3, respectively. The dam is defined by a black triangle. (b) Depth profile and (c) width profile (m) along the entire channel (km) obtained by the nautical chart of 2019 developed by the Hydrographic Institute of the Spanish Navy. The dashed gray lines represent the position of each sampling point.

The GRE is highly valued for its rich biodiversity and serves as a critical habitat for several economically important marine species. It plays a crucial role in feeding coastal areas along the Gulf of Cadiz, promoting high levels of primary productivity in the region (Ruiz et al., 2015; Cañavate et al., 2021; Bermudez et al., 2021). However, it is also a source of economic and environmental conflict due to the coexistence of multiple activities (salt production, agriculture -especially rice, which requires large amounts of water fishing- and navigation). Extensive human modification of the estuary has led to a significant reduction in the original marshes and a reduction in their original length to accommodate agricultural and navigation needs (Ruiz et al., 2017). This high anthropogenic pressure has caused changes in both the hydrodynamics and morphology of the system, favoring the constant degradation of the ecosystem (López-Ruiz, 2012; Zarzuelo et al., 2017).

This estuary has been extensively studied in terms of chemical contamination (e.g. Grimalt, 1999; Gomez-Parras et al., 2000; Riba et al., 2002) and fisheries (e.g. Baldó and Drake, 2002; Fernández-Delgado et al., 2007; González-Ortegón et al., 2012). Other studies have focused on biogeochemical aspects (e.g. Navarro et al., 2011; Ruiz et al., 2013, 2015, 2017; Huertas et al., 2018) and microplastic transport (Bermudez et al., 2021). However, only a few studies have focused on the hydrodynamic aspects (Álvarez et al., 2001; Diez-Minguito et al., 2012, 2014; or Losada et al., 2017). According to Siles-Ajamil et al. (2019), using a linearized multichannel analysis model, an increase in the mean channel depth leads to both

https://doi.org/10.5194/egusphere-2024-2451
Preprint. Discussion started: 7 August 2024

increased tidal height and saltwater intrusion. In a more recent study, Sirviente et al. (2023) used numerical simulations to show a significant current amplification of the M2 tidal wave at the head of the estuary. This amplification exceeded the amplitude of the wave at the mouth of the estuary due to channel deepening. The authors also showed altered tidal current dynamics characterized by increased intensity at the mouth of the estuary, potentially leading to greater intrusion of the salt wedge.

Salinity is the main environmental factor determining the spatial distribution of species in estuaries (Marshall and Elliott, 1998). Therefore, it is essential to have a clear understanding of the behaviour of this variable. In the GRE, salinity presents a clear horizontal gradient that decreases upstream (Gonzalez-Ortegon et al., 2014). Regarding salinity structure, the decrease in freshwater flows in the GRE has triggered gradual salinization of the system. Based on data from a real-time monitoring network (Navarro et al., 2011), Díez-Minguito et al. (2013) found that salinity distribution is controlled by nontidal transport, Stokes transport, and tidal pumping. These authors suggested that the effective longitudinal dispersion coefficient is dependent on the length of the system, with a higher mean value upstream. They also analysed the estuarine recovery response to strong discharge conditions (usually short but intense regimes), proposing that the displacement of saline intrusion towards the mouth causes an increase in stratification. The authors proposed a net propagation speed of 4 cms-1 for the saline front within the estuary.

Reyes-Merlo et al. (2013) assessed the relative influence of climatic forcers (freshwater discharge, tidal currents, and wind) on saltwater intrusions in the GRE using Markov chain Monte Carlo simulations. They argued that under low-flow regimes, wedge intrusion depends more on mean tidal fluctuations than on river discharge. They also proposed tidal pumping and baroclinic circulation as the drivers of salt transport. Their results indicate that the duration of salt intrusion would increase by approximately 8% under the expected scenario of a 15% decrease in freshwater discharge over the next 15 years.

Using an analytical model, Siles-Ajamil et al. (2019) explored the effects of management alternatives on salinity distribution, with channel deepening and marsh recovery potentially affecting tidal wave propagation and salinity. The authors argue that the mean salinity distribution shifts upstream, increasing the maximum salinity gradient, salinity intrusion, and M2 tidal salinity generated by the advection of the mean salinity gradient. These studies collectively highlight the dynamic nature of salinity in the Guadalquivir Estuary, influenced by both natural and human factors. However, there is a lack of information on the temporal and spatial variability of the salt wedge in the GRE, as well as the impact of anthropogenic pressures. Constant dredging (Gallego and García-Novo, 2006; Donázar-Aramendía et al., 2018) and cultivation fields over the last decade have caused changes in the behavior of the salt wedge. This, coupled with the limited contribution of freshwater from the dam (Contreras and Polo, 2012), leads to high salinity levels in the upper reaches of the river.

According to Algaba et al. (2024), the primary water abstractions in the Guadalquivir River basin are irrigation (88%), domestic uses (10%), industrial activities (1.1%), and energy production (0.9%). This indicates that the Guadalquivir basin is subject to constant human pressure, which modifies the ecological flow rate of the system. Therefore, it is necessary to characterize the actual state of the salinity wedge and the effects of anthropogenic pressure on the GRE.

https://doi.org/10.5194/egusphere-2024-2451
Preprint. Discussion started: 7 August 2024

Obtaining in situ measurements over time and space is a challenging task that is often not feasible. Therefore, numerical simulations capable of replicating the current state of estuarine salinity intrusion are essential for understanding the system and developing management strategies for its preservation.

This manuscript provides an analysis of the current state of salinity intrusion in the GRE and evaluates the impact of anthropogenic pressures on the behavior of the salt wedge. For the first time, the effect of anthropogenic water subtractions in modifying the estuary hydrodynamics and the associated salt wedge penetration will be analysed. To achieve this, we used a realistic 1D model which includes a hydrodynamic module (Sirviente et al., 2023) and a salt transport-dispersion module. This model was calibrated and validated using observations gathered during multiple oceanographic campaigns conducted from 2021 to 2023. Measurements were taken continuously during both upstream and downstream voyages of the ship, with sampling points along the river monitored over different time coverage (hours to days). We conducted various numerical experiments, designing scenarios with different freshwater inputs and degrees of anthropogenic water withdrawals, to perform a comprehensive simulation-based analysis.

2.Methodology

The analysis is based on a 1D hydrodynamic model capable of realistically simulating tidal-fluvial dynamics (sea surface elevation and current velocity), coupled with a transport and dispersion model to simulate salt concentration fields within the GRE. The hydrodynamic module has been previously calibrated and validated with high reliability (Sirviente et al., 2023). This manuscript focuses on the calibration and validation of the salt transport and dispersion module. For this purpose, in situ observations gathered from multiple short-duration oceanographic campaigns conducted during the dry seasons from 2021 to 2023 will be used. Once calibrated and validated, the model is used to analyze salt intrusion behavior under different freshwater flow and anthropogenic pressure scenarios (section 3). Anthropogenic pressures are defined as reductions in the water volume of the estuary (sinks) caused by diverse anthropogenic uses, such as water use in adjacent crop fields, losses associated with the flow modification in the channels or avenues of the estuary or illegal wells.

2.1. Data source

During the years 2021, 2022 and 2023, several oceanographic campaigns were conducted along the GRE during dry months (low or negligible rainfall and reduced freshwater flow). These short-term campaigns provided observations at different times along the river (Table 1). Measurements were obtained from a conductivity sensor installed on the oceanographic vessel UCADIZ, which recorded data every minute as the ship traveled upstream the GRE (MG1, from km 5 to km 73; MG2, from km 5 to km 73; MG3, from km 5 to km 60; MG4, from km 5 to km 80) and downstream the GRE (MG3, from km 10 to km 58; MG4, from km 7 to km 65) . This validation strategy, which will be further justified in section 3.1, allowed for simultaneous validation of the simulation outputs in both space and time. Additionally, short-term observations collected from moorings at different locations (Fig. 1a) were analyzed to validate the time variability of the simulations throughout the

https://doi.org/10.5194/egusphere-2024-2451
Preprint. Discussion started: 7 August 2024

tidal cycles at various points along the river. Specific sample points, dates, and time lengths of the observations are detailed in Table 1.

Table 1: Information about the salinity data (psu) records collected along the Guadalquivir Estuary during different oceanographic campaigns. The sample point locations are shown in Fig. 1a. The temporal resolution of each measurement is indicated as Δt. "Up" and "down" of vessel trips refer to upstream (from Xo to the dam) and downstream (from the dam to Xo) of the GRE.

Campaign	Station	Date	Time-interval	Δt
MG1	Vessel trip (up)	20/09/2021	5h	Minute
	MG1 P1	21/09/2021	9h	Hour
	MG1 P2	23/09/2021	10h	Hour
	MG1 P3	24/09/2021	10h	Hour
MG2	Vessel trip (up)	31/01/2022	6h	Minute
	MG2 P1	01/02/2022	10h	Hour
	MG2 P2	02/02/2022	10h	Hour
	MG2 P3	03/02/2022	10h	Hour
	MG2 P4	04/02/2022	10h	Hour
	MG2 P5	05/02/2022	9h	Hour
MG3	Vessel trip (up)	19/07/2022	6h	Minute
	Vessel trip (down)	20/07/2022-21/07/2022	4h	Minute
	MG3 P1	19/07/202-20/07/2022	25h	Hour
	MG3 P2	20-07/2022-21/07/2022	25h	Hour
	MG3 P3	21/07/2022-22/07/2022	11h	Hour
MG4	Vessel trip (up)	17/10/2023	8h	Minute
	Vessel trip (down)	18/10/2023	4h	Minute

2.2. Numerical hydrodynamic module description

The hydrodynamic module used in this study was described, calibrated, and validated by Sirviente et al. (2023). This 1D module integrates a system of long-wave equations along an elongated channel (Godin and Martinez, 1994)

$$\frac{\partial u}{\partial t} + u\frac{\partial u}{\partial x} = -g\frac{\partial \eta}{\partial x} - \frac{k|u|u}{(h+\eta)} \quad , \tag{1}$$

$$\frac{A}{h}\frac{\partial \eta}{\partial t} = -\frac{\partial}{\partial x}[Au] \quad , \tag{2}$$

The first equation represents the balance of along-channel forces, while the second ensures volume conservation. Here, u represents along-channel current velocity (ms^{-1}), t denotes time, x denotes the along-channel position (m), k is the bottom

https://doi.org/10.5194/egusphere-2024-2451
Preprint. Discussion started: 7 August 2024

friction coefficient (k = 0.003), η is sea level elevation above mean sea level (m), h (m) denotes average bottom depth across the channel below mean sea level, b represents the across- channel width, and $A = (h + \eta)b$ is the instantaneous cross-sectional area across the channel. The spatio-temporal distributions of η and u variables were derived by the numerical integration of these equations using an explicit finite differences scheme (leapfrog type) (Dronkers, 1969).

The GRE is assimilated to a 110 km channel extending from its mouth ($x = 0$) to the head ($x = L$). For the numerical integration of the independent variables (x, t), the values Δx = 25 m and Δt = 1 s are set, yielding a Courant-Friedrichs-Lewy coefficient of 0.39, which ensures numerical stability.

The channel cross-sections are approximated by rectangles, where the sides are defined by the across-channel averaged bottom depth $h(x)$ and channel breadth $b(x)$. Sea level predictions, based on harmonic constants derived from the harmonic analysis of sea level during 2019 at Bonanza station (data provided by *Puertos del Estado*, PdE), were used to force the simulation at the open boundary near Bonanza (Fig. 1a). A no-flow boundary condition normal to the section of the *Alcalá del Río* dam was also prescribed. The module considers the contributions from three tributary flows, A33 (*Rivera de Huelva*), H09 (*Alcalá del Río*), and A50 (*Zufre*), whose flow rates are not negligible. Hourly data of the tributary flows, covering the 7 days of simulation for each campaign (sections 2.1 and 2.2) and 15 days (for section 2.3) were provided by the Guadalquivir Hydrological Confederation (Guadalquivir SAIH, https://www.ch guadalquivir.es/saih/, last access: 25 March 2024).

To account for water volume withdrawals from the estuary, a parameter called "sink" (denoted by δ) was introduced. It represents the thickness (meters) of a water slide of horizontal area equal to $b \cdot \Delta x$, the horizontal area contained between each pair of transversal sections. This parameter is subtracted at each integration time step Δt from the previously computed η value. This is equivalent to withdrawing a water volume $b \cdot \Delta x \cdot \delta$ at each integration time step Δt. The suitable value of δ for each pair of transversal sections is determined together with the validation of the salt transport and dispersion model, as explained in section 3.1.

The bathymetry used is the most recent, obtained from the 2019 nautical chart produced by the Hydrographic Institute of the Spanish Navy (*Instituto Hidrográfico de la Marina*, IHM). This information was used to determine the average depth and breadth of the transverse channel at each of the equally spaced transverse sections of the GRE, with a distance of Δx = 25m between sections.

2.3. Numerical Transport and dispersion module description

A one-dimensional transport and dispersion module was developed to simulate the evolution of salt concentration within the estuary. To discretize the advection and diffusion terms with respect to space and time, a numerical integration of the channel-averaged 1D transport equation Eq. (3) was used based on the Multidimensional Positive Definite Advection Transport Algorithm (MPDATA) (Smolarkiewicz and Margolin, 1998), which is a type of finite-difference approximation used for advective terms in fluid equations that preserves the monotonicity of the solution. The technical characteristics of

https://doi.org/10.5194/egusphere-2024-2451
Preprint. Discussion started: 7 August 2024

the algorithm make it suitable for problems involving complex geometries and inhomogeneous flows (Smolarkiewicz and Szmelter, 2005).

$$\frac{\partial}{\partial t}(AS) + \frac{\partial}{\partial x}(AuS) = D\frac{\partial}{\partial x}\left[\frac{\partial}{\partial x}(AS)\right], \quad (3)$$

where S is the salinity concentration (psu); t is the time coordinate; x is the along-channel coordinate (m); u is the along-channel current velocity (ms^{-1}), D is the turbulent diffusion coefficient (m^2s^{-1}); $A = (h + \eta)b$ is the instantaneous across-channel section, where η is the sea level elevation above the mean sea level (m), h (m) is the across-channel averaged bottom depth below the mean sea level, and b is the cross channel width.

The sea level elevation (η) and current velocity (u) were simulated by the hydrodynamic module and implemented as inputs in the transport module, thus developing a 1D model for GRE.A free transmission condition ($\frac{\partial^2 S}{\partial x^2} = 0$) at the open boundary and a reflection condition ($\frac{\partial S}{\partial x} = 0$) at the channel edge were imposed as boundary conditions.

As an initial condition for the numerical integration, a salinity profile following a logistic function was established. This was unique for each simulation according to the characteristics of the observations, starting all of them from a value of 36 psu at the mouth and becoming 0, starting at km 85 until km 110. Likewise, the module was forced in a section near Bonanza (Fig. 1a), specifying an appropriate temporal variation of the salinity calculated as a function of the current (u) in this section and derived from the available observations.

After extensive calibration with salinity observations, a constant value of D = 0.5 m2s-1 was established along the channel. Additionally, as previously mentioned, a logistic approximation was used as the initial condition. Due to the variable conditions of the system, it is crucial to define a curve for each campaign (due to the high variability involved throughout different months and years). This curve is adjusted using the salinity observations to obtain the optimal curve where the model remains stable over time and space. During this calibration process, sink values are also determined for each observation. Numerous sink values are tested, ranging from 0 mm to 1 cm, with the chosen value being the one whose resulting simulation most closely resembles the observations.

3.Results and discussion

In this section, the main results obtained with the numerical model are presented, focusing on evaluating the dynamics of salinity intrusion in the GRE. As previously mentioned, the hydrodynamic module validation can be found in Sirviente et al. (2023). Initially, the outcomes from the experimental validation are presented. Subsequently, numerical experiments were conducted to assess the impact of salinity intrusion resulting from changes in freshwater inflow and in water volume along the GRE.

https://doi.org/10.5194/egusphere-2024-2451
Preprint. Discussion started: 7 August 2024

3.1. Experimental validation of the salt transport and dispersion model.

During the model validation phase, it was found that the penetration of the salt wedge into the interior of the estuary coming from the data measurements was much greater than those simulated using only the flow data provided by official sources. Hence, we became aware that significant undocumented water withdrawals were occurring during the different campaigns. Such withdrawals may be attributable to the utilization of estuarine water by neighboring crop fields, illegal wells and the filling of small channels and tributaries.

We addressed this issue by introducing a water volume withdrawal along the estuary (sinks) that allows the salinity shown by the observations to be adjusted. As mentioned earlier in the description of the hydrodynamic module, these volume withdrawals are denoted by the sink parameter δ

Considering that the intensity, spatial location, and temporal variability of these withdrawals are unknown, the numerical models had to undergo an ad hoc experimental validation for each campaign (MG1, MG2, MG3, and MG4). For each numerical integration, an initial salt concentration field was defined using a logistic function that was determined by the behavior of the observations. The procedure begins by establishing a δ value in the hydrodynamic model, running the model, and later using the resulting u and η outputs in the salt transport and dispersion model to fit the salinity observations. This procedure was repeated as many times as necessary until reaching the best fit to the salinity observations.

The experimental validation determined that the best fitting of the simulated salinity values to the observations are those presented in the following lines. For MG1, a δ = 0.0475 mm was applied uniformly from km 0 to km 10 and then decreased to 0.0275 mm for the remaining sections. In MG2, a constant sink of 0.0250 mm per unit area was implemented in all sections except for km 25-60, where it was increased to 0.0295 mm. In MG3, a uniform sink of 0.0225 mm was employed throughout all the sections. Finally, for MG4, a constant sink of 0.0220 mm was adopted across all sections except for km 40-70, where it increased to 0.0385 mm. The slightly higher sinks in the first 20 km of the estuary can be justified by the presence of the marshes of the Doñana Natural Park. Similarly, those simulations where a higher sink factor was used between km 30 and km 50 can be justified by the location of crop fields (Fig. 1a)

Fig. 2 shows the behavior of the longitudinal observations collected. In general, the simulations can reproduce the observations with high accuracy. The most significant discrepancies were identified in MG1 (Fig. 2a), within the first 6 km, where the model overestimated the salinity concentration. This also occurred between 35 and 50 km, indicating an underestimation. The MG2 simulation (Fig. 2b) shows the best fit, with a slight underestimation from 10 to 15 km. MG3 and MG3_B (Figs. 2c and d) correspond to observations collected on consecutive days. A good agreement between observation and simulation can also be observed for the whole channel. An overestimation in MG3 was found near the mouth (km 4), and from km 30 to km 40 the model slightly underestimated the concentration. This last underestimation was also observed for MG3_B. Finally, MG4 and MG4_B (Figs. 2e and f) show the largest differences. Although all the analyzed observations correspond to the low-flow regime ($\overline{Q}_{MG1}$ = 8 m^3s^{-1}, $\overline{Q}_{MG2}$ = 12 m^3s^{-1}, $\overline{Q}_{MG3}$ = 8 m^3s^{-1}), these campaigns are the ones with the lowest flow, which was practically negligible ($\overline{Q}$ = 3 m^3s^{-1}). For MG4 (Fig. 2e.), The simulation shows small oscillations

https://doi.org/10.5194/egusphere-2024-2451
Preprint. Discussion started: 7 August 2024

that slightly overestimate and underestimate the signal until km 50, where the curve drops and an underestimation of 3 psu was obtained. Similarly, for the consecutive day MG4_B (Fig. 2f), an overestimation not exceeding 3 psu was obtained along the entire estuary until km 57, where the simulation drops, causing an underestimation of the concentration in the upper part of the estuary.

The differences between simulations and observations near the mouth of the estuary can be explained by their proximity to the model boundary conditions, which generate a disturbance that can add noise in the first kilometers of the simulation. The discrepancies found between km 30 and 50 can be attributed to the crop fields adjacent to the channel. The November 2023 observations show interesting results; they represent very high values of salinity in the upper part of the estuary, reaching salinities of 5 psu at km 70. These high concentrations are anomalous and could be caused by eventual stronger water withdrawals further along the river.

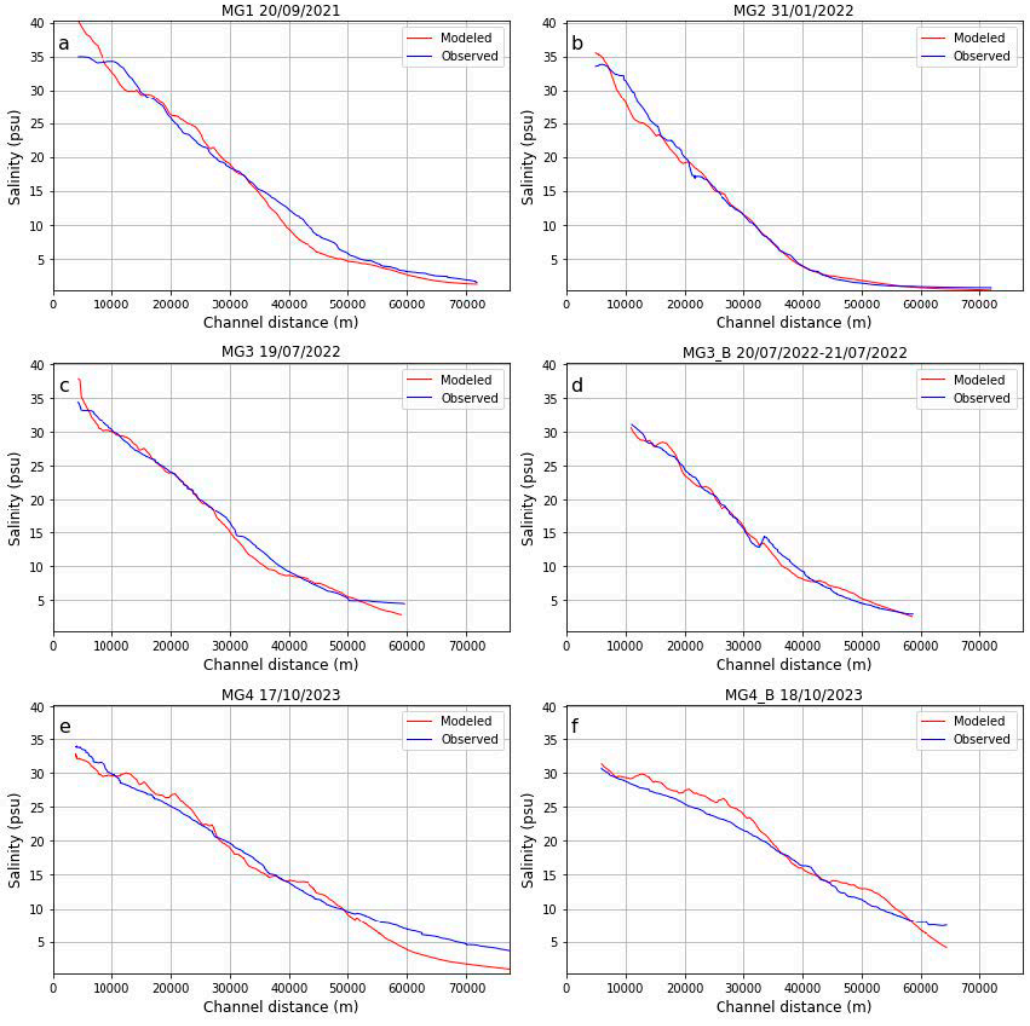

Figure 2: Comparison between the observations (blue line) and the simulation (red line) of the salinity (psu) for the hole channel for different campaigns (Table 1).

https://doi.org/10.5194/egusphere-2024-2451
Preprint. Discussion started: 7 August 2024

The good agreement between observations and simulations is shown in Table 2. Correlation coefficients higher than 0.95 are obtained for all simulations, along with small root mean square errors (RMSE). The Nash-Sutcliffe Efficiency Coefficient (NSE) is used to evaluate the variability of the observations explained by the simulation. Values close to 1 indicate that the model is able to reproduce the observations. Similarly, the inequality between the series has been assessed as not significant, indicating that there are no significant differences between them (t-student, Table 2). Therefore, it can be said that the transport model can reproduce the salt concentration along the Guadalquivir with high reliability.

Table 2: Determination coefficient at 95% of confidence level, root mean square error (RMSE) for salinity (psu), Nash-Sutcliffe efficiency coefficients, and t-student values for each oceanographic campaign.

Campaign	R^2 (P_{value} 0.0)	RMSE	NSE	P value (t-student)
MG1	0.99	1.61	0.98	0.61
MG2	0.99	0.87	0.99	0.78
MG3	0.99	0.98	0.99	0.69
MG3_B	0.99	0.82	0.99	0.97
MG4	0.98	1.81	0.96	0.34
MG4_B	0.97	1.66	0.95	0.35

Based on the analysis of the data from the different stationary sampling stations, it can be inferred that there is a strong relationship between the two sets of data. This is evident from the high coefficients of determination obtained for the measurements taken at MG3 P1, MG3 P2 and MG3 P3 (see Fig. 1), which were all greater than 0.90. The RMSE for each sample were also relatively small (see in Supplementary Material SM1). Furthermore, similar good agreement was obtained for stations MG2 P1 to MG2 P5 (Fig. 1), with R2 values greater than 0.80 and RMSE errors less than 2 psu. However, for the sample points of MG1 (Fig. 1), the coefficients of determination were lower (R2 values greater than 0.75), and the RMSE were higher (values less than 2.5 psu) for all stations (SM2 and SM3, respectively). At stations MG1 and MG2, the model underestimated the signal, with smaller differences observed at stations in the upper and middle parts of the estuary and larger differences at stations in the lower part of the GRE.

It is worth noting that the introduction of sinks into the model provides only a rough approximation of the actual way in which withdrawals occur on both spatial and temporal scales. These sinks, which are assumed to occur at a constant rate over time, only partially resolve this uncertainty. The actual volume of water removed is unknown. This uncertainty may be behind this slight underestimation of the model. Other sources of uncertainty could be the salinity increases caused by drainage from the marshes to the channel mouth. These waters, enclosed in extremely shallow marshes, may experience salinity increases due to evaporation before being discharged into the estuary. In addition, water drained from crop fields, such as during rainy periods, can bring additional concentrations of salts due to the presence of fertilizers carried by the water from the soil of the crop fields. Despite this, considering the overall consistency of the validations and statistical analyses, we can assert that the model demonstrates a good level of reliability in reproducing the salinity variations.

https://doi.org/10.5194/egusphere-2024-2451
Preprint. Discussion started: 7 August 2024

3.2. Salt wedge behaviour in the observation campaigns.

Figs. 3a-d display the salinity at 2 m depth recorded by the thermosalinograph of the vessel while sailing along the estuary in the center of the channel in September 2021 and January 2022 (Table 1). As illustrated, the salinity intrusion extends beyond km 30 in both cases, exceeding 20 psu at km 20. The highest concentrations are found at the mouth of the estuary, with values close to 36 psu. This observation confirms the basic premise of our modelling approach, in which we incorporate an initial condition by imposing a temporal salinity fluctuation calculated as a function of current velocity. This is based on the salinity benchmark of 36 psu at the open sea mouth. In September 2021 (Fig. 3a), concentrations below 5 psu are obtained from approximately km 50 onwards, while for January 2022 (Fig. 3d), these concentrations are observed from km 40 onwards.

Model simulations that included water withdrawals (Figs. 3b-e) closely resembled the observed behavior of the salinity intrusion. In general, simulations including this factor can effectively replicate the observed salinity. However, when sinks were not considered (Figs. 3c and f), the simulated salinity was significantly lower than the observed values. Note that concentrations of practically 0 psu were obtained from km 25 onwards. This configuration could be regarded as the natural state of the saline wedge, unaltered by anthropogenic intervention.

These results remained consistent throughout all the comparisons with experimental data examined (shown in Fig.SM4 and SM5). At this point of the analysis, on the one hand it is clear that including these water sinks is necessary to simulate a realistic salt transport throughout the GRE. On the other hand, the existence of these sinks reveals the significant impact that the usage of water, such as those demanded by the adjacent crop fields or other domestic needs, may have on the saline wedge penetration. It is important to note that even though the actual consumption and consumers of the estuarine water remain unknown, the model has detected that a clear deficit of water had been produced in the estuary during the analyzed periods. As previously pointed out, a penetration of the salinity wedge beyond 25 km from the mouth would not occur if the consumed water had been compensated with an increased flow from the dam. In this sense, the applied analysis methodology could be used to check, using the vessel-based observations and the described numerical simulations, the degree of alteration of the salinity wedge location in a given epoch, using the location of the simulated salinity wedge corresponding to the absence of sinks as a reference.

https://doi.org/10.5194/egusphere-2024-2451
Preprint. Discussion started: 7 August 2024

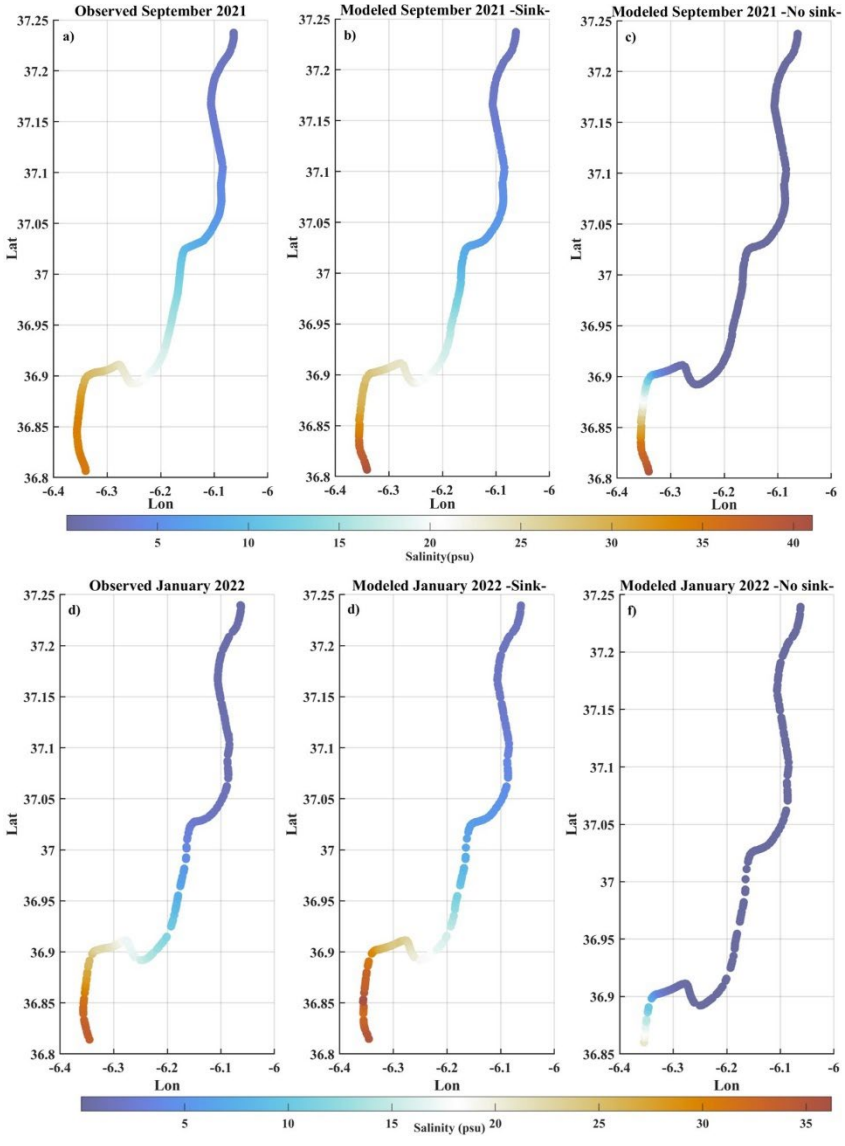

Figure 3: Salinity concentration maps (psu) of the Guadalquivir River Estuary from the oceanographic campaigns MG1 and MG2 on 20/09/2021 (a, b, c) and on 30/01/2022 (d, e, f), respectively. Observational data are shown in (a) and (d). Simulation including water volume reductions are presented in (b) and (e). (c) and (f) correspond to model simulation without sinks.

3.3. Tidal cycle dynamics.

Once the reliability of the model had been confirmed by the results of the experimental validation presented in the previous sections, it was used to simulate the dynamic of the salt wedge during a spring-neap tidal cycle. To do this, we conducted a simulation extended over 15 days (15/07/2022-30/07/2022). This period was selected because it comprised records of observations distributed throughout the spring-neap tidal cycle, allowing for the validation of the simulations.

https://doi.org/10.5194/egusphere-2024-2451
Preprint. Discussion started: 7 August 2024

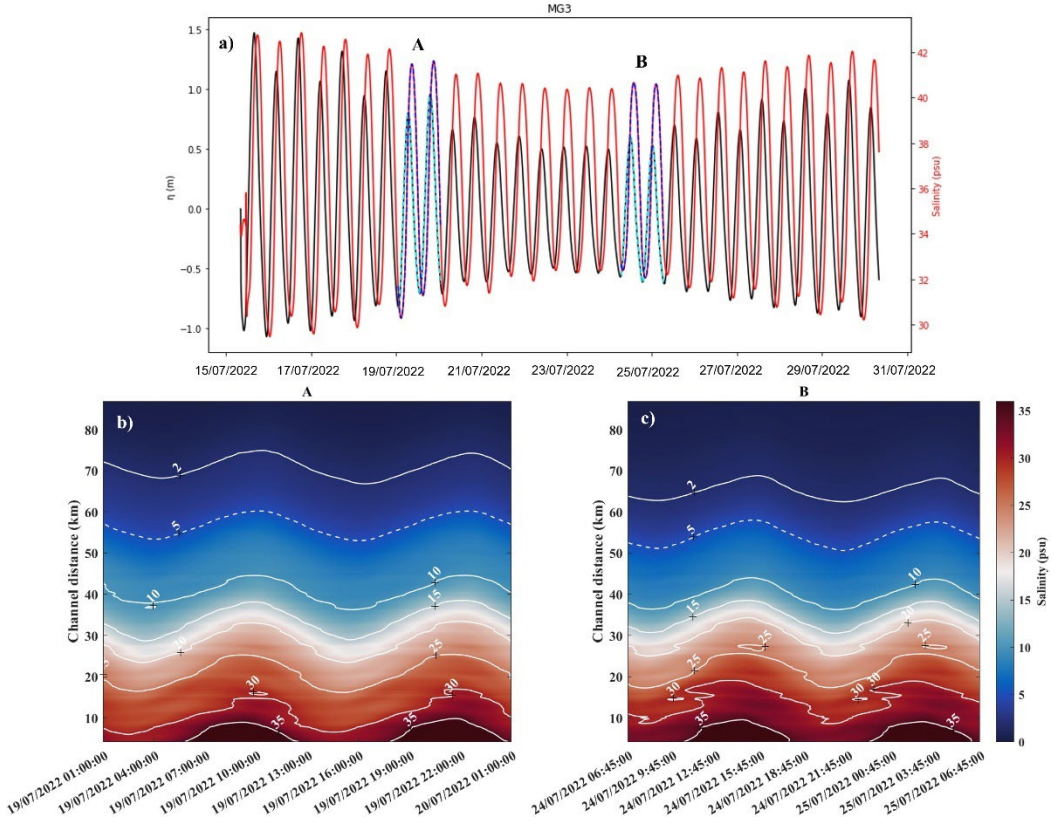

Figure 4: (a) Superposition of tidal height (m) and salinity (psu) simulated time series at Bonanza section throughout 15 days of July 2022. Dashed lines indicate the selected 24 h periods referred to in Figs. 4b and 4c; Hovmöller diagrams of simulated salinity variation over these two daily cycles (24 h) during periods just after spring tides (b) and neap tides (c) along the Guadalquivir estuary.

We focused on two 24-hour periods to describe the behavior of saline intrusion dynamics during different stages of the semidiurnal cycle (Fig. 4a). An approximate 1.5-hour lag between tidal height and salinity profiles was observed, also a gradual decrease in salinity values upstream can be seen. The maximum and minimum extent of the saline wedge within the channel coincided with moments just before high and low tides, respectively.

Fig. 4b shows the progression of the saline wedge during the first intermediate tide (A) following spring tides. Notably, during the flood tide, the wedge demonstrates minimal intrusion into the estuary, with the 5 psu isohaline confined below km 53. Conversely, during the ebb tide, the maximum saline intrusion occurred, exceeding over 60 km along the 5 psu isohaline. This highlights a difference of about 10 km in the salt front between the ebb and flood tides, using the 5 psu isohaline as a boundary. For the second period, B (Fig. 4c), which corresponds to intermediate tides immediately after neap tides, slightly lower salinity concentrations are observed. The maxima of the 5 psu isohaline are found at km 58, and minima does not extend beyond km 50. The most significant differences were observed in the 2 psu isohaline, with differences of 6 km between periods A and B. This suggests that during spring tides, the salt wedge reaches higher concentrations upstream compared to neap tides. Moreover, it can be speculated that the discrepancies between spring and neap tides for the 2 psu

https://doi.org/10.5194/egusphere-2024-2451
Preprint. Discussion started: 7 August 2024

isohaline would exceed 6 km. This finding is consistent with the results suggested by Díez-Minguito et al. (2013), who documented a net displacement of approximately 10 km between spring and neap tides.

The system is unable to expel the saline wedge during the low freshwater regime, resulting in the formation of a saline plug at the estuary's mouth. This prevents the outflow of internal waters towards the continental shelf of the Gulf of Cadiz, potentially affecting water quality and species in the estuary. This conclusion is supported by the positive mass balance at the estuary's mouth (185.41 m^3s^{-1}).

These results suggest that the constant anthropogenic pressure on the estuary has caused a change in saline intrusion, resulting in higher salinity levels upstream of the river compared to the records of previous studies, such as that of Fernández-Delgado et al. (2007). In this study, it was found that over a six-year period (1997–2003), the 5 psu isohaline boundary was located near km 25 at low tide and at km 35 at high tide. The 18 psu isohaline limit was also found to be 5 km and 15 km upstream of the river mouth at low and high tides, respectively.

4. Discussion of the main anthropogenic pressures driving salt wedge penetration.

The natural flow regime of the Guadalquivir estuary has undergone significant changes due to different human activities in the basin (Bramato et al., 2010). Agricultural activities, land demand, and the channelization of the estuary for navigation purposes have collectively contributed to significant changes in its geomorphology (Ruiz et al., 2015). The construction of the *Alcalá del Río* dam has affected tidal propagation, and multiple water uses - including agriculture, human needs, and industry- have resulted in a 60% reduction of freshwater inflows (Contreras and Polo, 2010).

The results from previous numerical simulations clearly suggest that human activities (freshwater uses) developed in the estuary, along with the decrease in the freshwater inputs, are behind the excessive penetration of the salt wedge. It is not possible to reproduce the behavior of this wedge along the river without adding these effects. As previously mentioned, river discharges into estuaries are regulated mainly for economic reasons: power generation, irrigation, and freshwater supply to populations located near the basin (Vieira and Bordalo, 2000; Jassby et al., 2002). This freshwater use leads to a decrease in estuarine water volume and thus to increased salt intrusion. In recent years, freshwater discharges to the estuary have reduced by more than 50% on average, and during dry periods, freshwater input is almost completely controlled by the *Alcalá* dam (Baldo et al., 2005; Fernandez-Delgado et al., 2007).

The model used in the present study, which accurately reproduces the current salinity along the river, has shown that without the introduction of water sinks, the system would not achieve the salinity presented in the observations. This fact highlights the need to understand the effects that changes in the amount of these water withdrawals, along with changes in freshwater flow, could exert on the salt wedge behavior. For this purpose, different numerical experiments were designed for various freshwater flow and water sinks. The resulting simulations will be compared with those obtained in the two 2022 campaigns, MG2 and MG3 under the freshwater flow and sinks previously determined in section 3.

https://doi.org/10.5194/egusphere-2024-2451
Preprint. Discussion started: 7 August 2024

4.1. Changes in freshwater flows

The freshwater discharge observed in MG2 and MG3 are respectively Q = 12 m^3s^{-1} and Q = 8 m^3s^{-1}; these values were used as reference values. Five experiments were conducted under the following different freshwater flows:

i. Observed flow reduced by 50%.
ii. Observed flow set to zero.
iii. Observed flow increased by 50%.
iv. Observed flow increased up to 40 m^3s^{-1}, established as the low-flow condition, following Díez-Minguito et al. (2012).
v. An averaged flow of 185 m^3s^{-1}, following Costa et al. (2009) and Morales et al. (2020).

The resulting simulations were analyzed at two specific moments of the tidal cycle at Bonanza station: the maximum ebb current (E) and the maximum flood current (F), which closely correspond to maximum and minimum salt wedge intrusion, respectively. A 50% reduction in freshwater flow for the MG2 simulation barely differs from the current state (Fig. 5a, blue line), with a maximum difference of 0.6 psu for both tidal instances (E, F). The highest differences are found in the experiment (ii), where the freshwater flow is cancelled. As seen in Fig. 5a, maximum changes do not exceed 1.2 psu. The zone of highest salinity differences oscillates from km 10 to km 40. During maximum ebb current (just after low tides), when minimum salt wedge intrusion occurs, the zone with the highest differences (E -50% and E -100%) is within the first 20 km from the mouth. Conversely, during flood tides (just after high tides), the maximum salt intrusion is present, this zone moves by approximately 10 km with respect to the position in maximum ebb current. These results confirm those of section 3.3, showing a salt wedge displacement of about 10 km between maximum ebb and flood current. This behavior holds for both MG2 and MG3 cases.

https://doi.org/10.5194/egusphere-2024-2451
Preprint. Discussion started: 7 August 2024

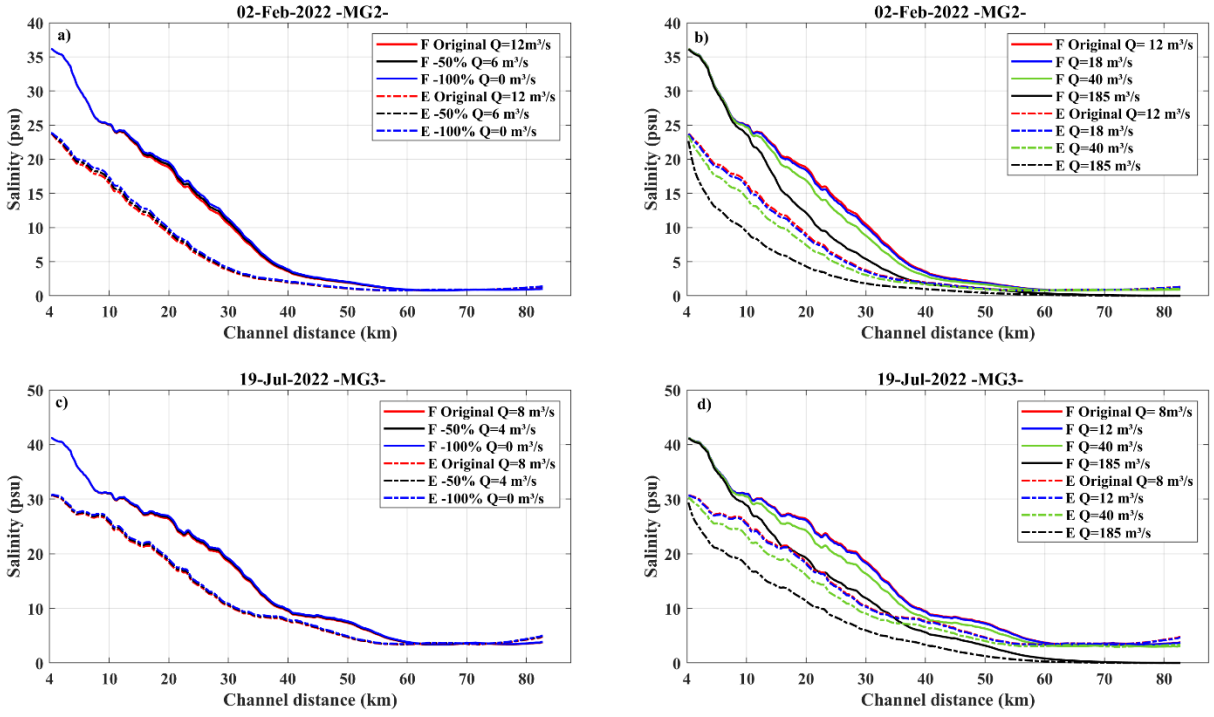

Figure 5: Series of salinity (psu) along the Guadalquivir estuary (km) between actual flow and various reductions in freshwater flow for MG2 (a) and MG3 (c) oceanographic campaigns. In a and c, the red lines represent the actual state, the black lines correspond to 50% reductions (i, m^3s^{-1}) and the blue lines to 100% reductions (ii). (b) and (d) are the series of actual flow and higher flows salinities for MG2 and MG3, respectively (50% increase -iii- represented by the blue line, a flow of 40 m^3s^{-1} -iv- by the green line, and a flow of 185 m^3s^{-1} -v- by the blackline). The solid lines represent the time of maximum salinity (F, Flood), and the dashed lines represent the time of minimum salinity (E, Ebb).

Greater differences were found in experiments (iii), (iv), and (v), where the responses, as expected, were reversed (Figs. 5b and 5d), indicating a reduction in the salt wedge penetration. Increasing the flow by 50% had no effect in any of the cases (MG2, MG3), with practically negligible differences (not exceeding 0.5 psu). However, a freshwater flow of 40 m^3s^{-1} produced a maximum difference of 2.5 psu, although these differences practically vanished 50 km upstream from the mouth. In addition, experiment (v) (Figs. 5b and 5d, black lines) shows the behavior of the salt wedge corresponding to yearly averaged freshwater flows. These experiments present the largest differences with respect to the reference periods. Differences up to 7 psu are obtained in the first 10 km for F (Q = 185 m^3s^{-1}) and in km 20 for E (Q = 185 m^3s^{-1}) in MG2 (Fig. 5b). For MG3, differences up to 8 psu are obtained for F (Q = 185 m^3s^{-1}) near km 10-20 and for E (Q = 185 m^3s^{-1}) between km 20-30 (Fig. 5d). In the upper part of the river, the salt concentration was lower, with differences of less than 2 psu. This indicates that under this flow condition, the estuary has a lower salt concentration along the estuary, showing that the salt wedge penetration is less pronounced in this freshwater regime than in the reference case.

https://doi.org/10.5194/egusphere-2024-2451
Preprint. Discussion started: 7 August 2024

These results suggest that, under conditions of high freshwater flows, the intrusion of the saline front from the Gulf is blocked by freshwater flow, resulting in a reduction in the salinization of the estuary. Low flow conditions prevail over 75% of the year (Díez-Minguito et al., 2012).

4.2 Changes in the water volume sinks.

To evaluate the effect of decreasing or increasing the sinks from GRE, four experiments were conducted, taking the sinks established in the validation of the numerical model for MG2 and MG3 campaigns as a reference:

i. Decrease by 15%.
ii. Decrease by 50%.
iii. Increase by 15%.
iv. Increase by 50%.

Reducing the sinks by 15% produces a decrease in salinity up to 5 psu for MG2 (Fig. 6a, black lines). Similarly, a greater reduction (50%, ii) of these sinks would result in a small salinity intrusion along the GRE, achieving differences of 15 psu (Fig. 6a, blue lines). It should be noted that the largest differences are obtained in the area with the greatest oscillation of the salt wedge, while small differences are obtained further upstream of this zone (Fig. 6a).

Conversely, an increase in the sinks leads to higher salinization of the estuary, especially in the inner part of the river. In Fig. 6b, it can be observed that increasing these sinks by 15% (experiment iii) results in an increase in salinity concentration of 10 psu. Likewise, under experiment (iii), an upstream shift of the saline front zone is obtained, reaching km 30 and km 40 at the moments of minimum (E) and maximum (F) penetration of the salt wedge, respectively. Similarly, if these sinks are further increased by 50%, as shown in experiment (iv), the estuary experiences an extreme salinization, with differences of nearly 40 psu.

Analogous results are obtained from the MG3 simulations (Figs. 6b and 6d), although the salinity differences are roughly halved compared to the MG2 results.

https://doi.org/10.5194/egusphere-2024-2451
Preprint. Discussion started: 7 August 2024

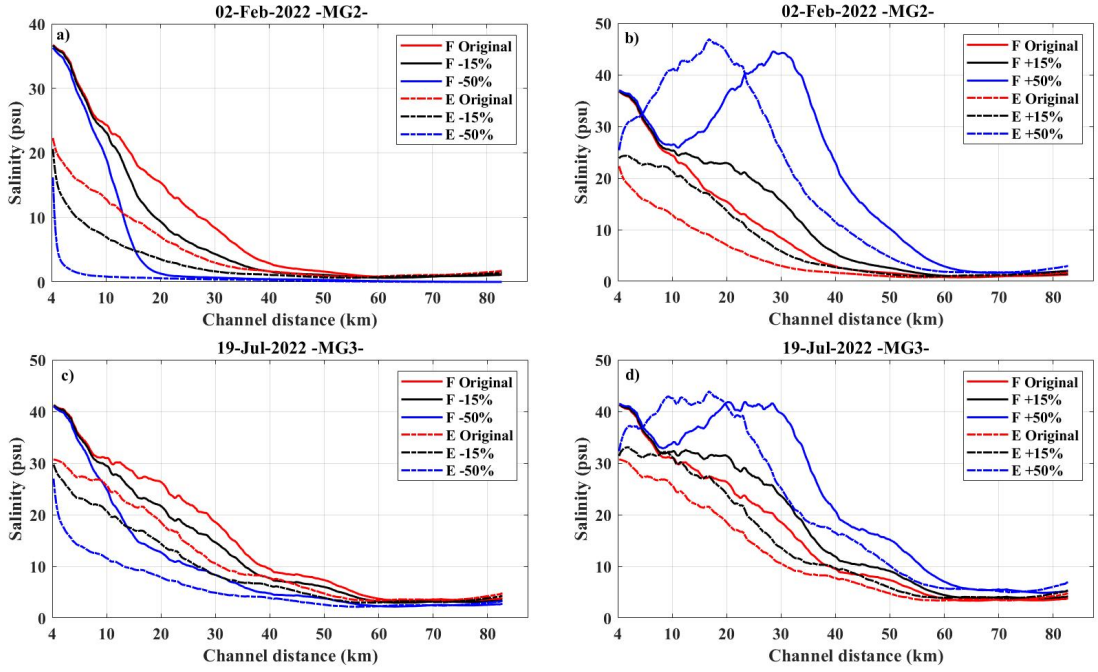

Figure 6: Series of salinity (psu) along the Guadalquivir estuary (km) of actual water sinks (red lines) and various reductions for MG2 (a) and MG3 (c) oceanographic campaigns. The black lines correspond to 15% reductions (m3s-1) and the blue lines to 50% reductions. Figures (b) and (d) correspond to salinity series of the actual water sinks (red lines) and an increase of 15% (black lines line) and 50% (blue lines). Solid lines represent the time of maximum salinity (F), and the dashed lines represent the time of minimum salinity (E).

These findings underscore the significant impact that changes in water volume sinks can have on the salinity dynamics of the Guadalquivir estuary. Reducing the sinks leads to a decrease in salinity, mitigating the extent of the salt wedge, while increasing the sinks exacerbates salinity intrusion, pushing the saline front further upstream. This sensitivity to water sinks emphasizes the importance of managing water usage to control salinity levels in the estuary, which is crucial for maintaining ecological balance and water quality.

5. Conclusions

The nonlinear 1D numerical model used in this study, which incorporates realistic variations in channel width and bottom depth (average values across the channel), as well as withdrawals originating from the system, has demonstrated a highly satisfactory performance achieved through an extensive process of calibration and validation. This process includes comparing simulations with numerous observations of salinity at various points along the estuary.

The changes in freshwater flow (Q) lead to slight variations in the current situation within the GRE. A decrease or increase in Q result in slight increases or decreases in salinity concentration. Significant reductions in saline intrusion were observed

https://doi.org/10.5194/egusphere-2024-2451
Preprint. Discussion started: 7 August 2024

only at moderate to high discharges (above 40 m^3s^{-1}). However, the main driver influencing the behavior of the salt wedge is anthropogenic water withdrawals from the estuary

The experiments conducted, though idealized, provide insight into the magnitude of anthropogenic pressures on the salinization of the GRE. The current state reveals an excessive penetration of the salt wedge into the GRE, as indicated by the transport and dispersion numerical model incorporating a sink parameter (δ) to simulate the effect of water volume withdrawals from the inner estuary. Thanks to this parameterization we can define a reference situation which would correspond to a situation where no sinks (δ=0) are considered. This reference situation would represent the ideal functioning of the estuary with a minimum penetration of the salt wedge that would never reach more than 25 km from its mouth.

The high salinity concentrations associated with the salt wedge have direct and detrimental impacts on the ecosystem. These impacts include altering water column properties such as turbidity, affecting primary production, and affecting crop fields and domestic water use. Moreover, these effects extend beyond the ecosystem to impact the ecosystem services and associated socio-economic aspects in this coastal area.

The changes in freshwater flow (Q) lead to slight variations of the current situation. A decrease/increase in Q slightly increases/decreases salinity concentration. Only at moderate to high discharges (above 40 m^3s^{-1}), was a significant reduction in saline intrusion observed. However, the main mechanism driving the observed behavior of the salt wedge is the anthropogenic water withdrawals from the estuary.

Furthermore, these effects of anthropogenic activities are not only limited to salinity. Upstream of the saline plug, various physicochemical and biological variables such as nutrients, organic matter, and contaminants could also accumulate. This plug will be only removed from the estuary under high discharge conditions, whereby a downstream current is generated. This in turn slows down the tidal flood currents, causing all accumulated substances at the mouth of the estuary to be exported into the Gulf of Cadiz.

Data availability. SAIH data are freely accessible via https://www.ch guadalquivir.es/saih/. Observational dataset and numerical simulations will be available in an online repository if the manuscript is accepted for publication.

Authors contribution. SS, MB planned and designed the study. SS has processed an analyzed the data. SS, JJG-P, MB-P, SS, JMS-P, and MB contributed with the analysis performance and interpretation of the results. MB revised the final version. SS has prepared everything.

Competing interests. The contact author has declared that none of the authors has any competing interests.

Acknowledgements. This work has been developed within the framework of the Spanish National Research Plan through the project TRUCO (RTI1018-100865-B-C22). Sara Sirviente was supported by a grant from the University of Ferrara and the University of Cadiz. Bolado-Penagos was supported by Plan Propio Investigadores Noveles UCA (BOLA642 PR2023-030) and the CEIMAR Jóvenes Investigadores (ASTRAL—CEI-JD-23-08).

https://doi.org/10.5194/egusphere-2024-2451
Preprint. Discussion started: 7 August 2024

References

Algaba, M.HP., Huyghe, W., van Leeuwen, K., Koop, S., and Eisenreich, S.: Assessment and Actions to Support Integrated Water Resources Management of Seville (Spain), Environ. Dev. Sustain., 26, 7347–7375, https://doi.org/10.1007/s10668-023-03011-8, 2024.

Álvarez, O., Tejedor, B., and Vidal, J.: La dinámica de marea en el estuario del Guadalquivir: un caso peculiar de resonancia antrópica, Física de la Tierra, 11–24, 2001.

Baldó, F., and Drake, P.: A multivariate approach to the feeding habits of small fishes in the Guadalquivir Estuary, J. Fish Biol., 61, 21–32, https://doi.org/10.1111/j.1095-8649.2002.tb01758.x, 2002.

Baldó, F., Cuesta, J.A., Fernández-Delgado, C., and Drake, P.: Efecto de la regulación del caudal del Río Guadalquivir sobre las características físico-químicas del agua y la macrofauna acuática de su estuario, Cienc. Mar., 31, 467–476, 2005.

Bermúdez, M., Vilas, C., Quintana, R., Gonzalez-Fernández, D., Cózar, A., and Díez-Minguito, M.: Unravelling spatio-temporal patterns of suspended microplastic concentration in the natura 2000 Guadalquivir (SW Spain): observations and model simulations, Mar. Pollut. Bull., 170, 112622. https://doi.org/10.1016/j.marpolbul.2021.112622, 2021.

Bramato, S., Contreras, E., Polo, M. J., and Losada, M. A.: An integrated database manager to forecast estuarine dynamics and water quality in the Guadalquivir river (Spain), River Flow 2010, 2,1415–1420, 2010.

Cañavate, J. P., Van Bergejik, S., González-Ortegón, E., and Vilas, C.: Contrasting fatty acids with other indicators to assess nutritional status of suspended particulate organic matter in a turbid estuary, Estuar. Coast. Shelf Sci., 254, 107239, https://doi.org/10.1016/j.ecss.2021.107329, 2021.

Contreras E., and Polo M. J.: Aportes desde las cuencas vertientes. Propuesta metodológica para diagnosticar y pronosticar las consecuencias de las actuaciones humanas en el estuario del Guadalquivir (in Spanish), technical report, Group of Fluvial Dyn. and Hydrol., University of Córdoba, Córdoba, Spain, 2010.

Contreras, E., and Polo, M. J.: Measurement frequency and sampling spatial domains required to characterize turbidity and salinity events in the Guadalquivir estuary (Spain), Nat. Hazards Earth Sys., 12, 2581–2589, https://doi.org/10.5194/nhess-12-2581-2012, 2012.

Costa, S., Gutiérrez Mas, J. M., and Morales, J. A.: Establecimiento del régimen de flujo en el estuario del Guadalquivir, mediante el análisis de formas de fondo con sonda multihaz, Rev. Soc. Geol. España, 22(1-2), 23-42, 2009.

Dauvin, J.-C.: Effects of heavy metal contamination on the macrobenthic fauna in estuaries: the case of the Seine estuary, Mar. Pollut. Bull, 57, 160–169, https://doi.org/10.1016/j.marpolbul.2007.10.012, 2008.

Díez-Minguito, M., Baquerizo, A., Ortega-Sánchez, M., Navarro, G., and Losada, M. A.: Tide transformation in the Guadalquivir estuary (SW Spain) and process-based zonation, J. Geophys. Res-Oceans, 117, C03019, https://doi.org/10.1029/2011JC007344, 2012.

https://doi.org/10.5194/egusphere-2024-2451
Preprint. Discussion started: 7 August 2024

Díez-Minguito, M., Contreras, E., Polo, M., and Losada, M. A.: Spatio-temporal distribution, along-channel transport, and post-river flood recovery of salinity in the Guadalquivir estuary (SW Spain), J. Geophys. Res-Oceans, 118, 2267–2278, https://doi.org/10.1002/jgrc.20172, 2013.

Díez-Minguito, M., Baquerizo, A., de Swart, H. E., and Losada, M. A.: Structure of the turbidity field in the Guadalquivir estuary: Analysis of observations and a box model approach, J. Geophys. Res-Oceans, 119, 7190–7204, https://doi.org/10.1002/2014JC010210, 2014.

Donázar-Aramendía, I., Sánchez-Moyano, J. E., García-Asencio, I., Miró, J. M., Megina, C., and García-Gómez, J. C.: Maintenance dredging impacts on a highly stressed estuary (Guadalquivir estuary): A BACI approach through oligohaline and polyhaline habitats, Mar. Environ. Res., 140, 455–467, https://doi.org/10.1016/j.marenvres.2018.07.012, 2018.

Fernández-Delgado, C., Baldó, F., Vilas, C., García-González, D., Cuesta, J.A., González-Ortegón, E., and Drake, P.: Effects of the river discharge management on the nursery function of the Guadalquivir River estuary (SW Spain), Hydrobiologia 587, 125–136, https://doi.org/10.1007/s10750-007-0691-9, 2007.

Gallego, J. B., and García Novo, F.: High-intensity versus low-intensity restoration alternatives of a tidal marsh in Guadalquivir estuary, SW Spain, Ecol. Eng., 30, 112–121, https://doi.org/10.1016/j.ecoleng.2006.11.005, 2006.

Godin, G., and Martinez, A.: Numerical experiments to investigate the effects of quadratic friction on the propagation of tides in a channel, Cont. Shelf Res., 14, 723–748, https://doi.org/10.1016/0278-4343(94)90070-1, 1994.

Gomez-Parra, A., Forja, J. M., DelValls, T. A., Sáenz, I., and Riba, I.: Early contamination by heavy metals of the Guadalquivir estuary after the Aznalcollar mining spill (SW Spain), Mar. Pollut. Bull., 40, 1115–1123, https://doi.org/10.1016/S0025-326X(00)00065-5, 2000.

Gomiz-Pascual, J.J., Bolado-Penagos, M., Gonzalez, C.J., Vazquez, A., Buonocore, C., Romero-Cozar, J., Perez-Cayeiro, M.L., Izquierdo, A., Alvarez, O., Mañanes, R., and Bruno, M.: The fate of Guadalquivir River discharges in the coastal strip of the Gulf of Cádiz. A study based on the linking of watershed catchment and hydrodynamic models, Sci. Total Environ., 795, 148740, https://doi.org/10.1016/j.scitotenv.2021.148740, 2021.

González-Ortegón, E., and Drake, P.: Effects of freshwater inputs on the lower trophic levels of a temperate estuary: physical, physiological or trophic forcing?, Aquat. Sci., 74, 455–469, https://doi.org/10.1007/s00027-011-0240-5, 2012.

González-Ortegón, E., Baldó, F., Arias, A., Cuesta, J. A., Fernández-Delgado, C., Vilas, C., and Drake, P.: Freshwater scarcity effects on the aquatic macrofauna of a European Mediterranean-climate estuary, Sci. Total Environ., 503–504, 213–221, https://doi.org/10.1016/j.scitotenv.2014.06.020, 2014.

Grimalt, J. O., Ferrer, M., and Macpherson, E.: The mine tailing accident in Aznalcollar, Sci. Total Environ., 242(1-3), 3–11, https://doi.org/10.1016/s0048-9697(99)00372-1, 1999.

Huertas, E., Flecha, S., Navarro, G., Perez, F. F., and De la Paz, M.: Spatio-temporal variability and controls on methane and nitrous oxide in the Guadalquivir Estuary, Southwestern Europe, Aquat. Sci., 80, 29, https://doi.org/10.1007/s00027-018-0580-5, 2018.

https://doi.org/10.5194/egusphere-2024-2451
Preprint. Discussion started: 7 August 2024

Jassby, A. D., Cloern, J. E., and Cole, B. E.: Annual primary production: patterns and mechanisms of change in a nutrient-rich tidal ecosystem. Limnol. Oceanogr., 47, 698–712, https://doi.org/10.4319/lo.2002.47.3.0698, 2002

Lopes, C. L., Le Fouest, V., Corzo, A., and Dias, J. M.: Editorial: Advances in monitoring and modelling spatial and temporal dynamics of estuarine ecosystems, Front. Mar. Sci., 11, 1367378, https://doi.org/10.3389/fmars.2024.1367378, 2024.

López-Ruiz, A., Ortega-Sanchez, M., Baquerizo, A., Navidad, D., and Losada, M. A.: Nonuniform alongshore sediment transport induced by coastline curvature, Coast. Eng, 1, https://doi.org/10.9753/icce.v33.sediment.29, 2012.

Losada, M.Á., Díez-Minguito, M., and Reyes-Merlo, M.Á.: Tidal-fluvial interaction in the Guadalquivir River estuary: spatial and frequency dependent response of currents and water levels, J. Geophys. Res-Oceans, 122, 847–865,https://doi.org/10.1002/2016JC011984, 2017.

Marshall, S., and Elliott, M.: Environmental influences on the fish assemblage of the Humber Estuary, U.K, Estuar. Coast. Shelf Sci., 46, 175–184, https://doi.org/10.1006/ecss.1997.0268, 1998.

Miranda, L. B., Andutta, F. P., Kjerfve, B., and Castro Filho, B. M.: Fundamentals of Estuarine Physical Oceanography (Vol. 8), Singapore, Springer., 2017

Morales, J. A., Carro, B. M., Sanmiguel, E. G., and Borrego, J.: Tasas de acumulación reciente en los márgenes del estuario del Guadalquivir, Geogaceta, 67, 2019.

Navarro, G., Gutierréz, F. J., Díez-Minguito, M., Losada, M. Á., and Ruiz, J.: Temporal and spatial variability in the Guadalquivir estuary: a challenge for real-time telemetry, Ocean Dynam., 61, 753–765, https://doi.org/10.1007/s10236-011-0379-6, 2011.

Reyes-Merlo, M. Á., Díez-Minguito, M., Ortega-Sánchez, M., Baquerizo, A., and Losada, M. Á.: On the relative influence of climate forcing agents on the saline intrusion in a well-mixed estuary: Medium-term Monte Carlo predictions, J. Coast. Res., 65, 1200–1205, https://doi.org/10.2112/SI65-203.1, 2013.

Riba, I., DelValls, T. A., Forja, J. M., & Gómez-Parra, A.: Influence of the Aznalcóllar mining spill on the vertical distribution of heavy metals in sediments from the Guadalquivir estuary (SW Spain), Mar. Pollut. Bull., 44, 39–47, https://doi.org/10.1016/S0025-326X(01)00171-0, 2002.

Ruiz, J., Macías, D., Losada, M. Á., Díez-Minguito, M., and Prieto, L.: A simple biogeochemical model for estuaries with high sediment loads: application to the Guadalquivir River (SW Iberia), Ecol. Model., 265, 194–206, https://doi.org/10.1016/j.ecolmodel.2013.06.012, 2013.

Ruiz, J., Polo, M. J., Díez-Minguito, M., Navarro, G., Morris, E. P., Huertas, E., Caballero, I., Conteras, E., and Losada, M. Á.: The Guadalquivir estuary: A hot spot for environmental and human conflicts, Environ. Manage. Gov., 8, 199–232, https://doi.org/10.1007/978-3-319-06305-8_8, 2015.

Ruiz, J., Macías, D., and Navarro, G.: Natural forcings on a transformed territory overshoot thresholds of primary productivity in the Guadalquivir estuary, Cont. Shelf Res., 148, 199–207, https://doi.org/10.1016/j.csr.2017.09.002, 2017.

https://doi.org/10.5194/egusphere-2024-2451
Preprint. Discussion started: 7 August 2024

Siles-Ajamil, R., Díez-Minguito, M., and Losada, M. Á.: Tide propagation and salinity distribution response to changes in water depth and channel network in Guadalquivir River estuary: an exploratory model approach, Ocean Coast. Manage., 174, 92–107, https://doi.org/10.1016/j.ocecoaman.2019.03.015, 2019.

Sirviente, S., Sánchez-Rodríguez, J., Gomiz-Pascual, J. J., Bolado-Penagos, M., Sierra, A., Ortega, T., Álvarez, Ó., Forja, J., and Bruno, M.: A numerical simulation study of the hydrodynamic effects caused by morphological changes in the Guadalquivir River Estuary, Sci. Total Environ., 902, 166084, https://doi.org/10.1016/j.scitotenv.2023.166084, 2023

Smolarkiewicz P. K., and Margolin L. G.: MPDATA: A Finite-Difference Solver for Geophysical Flows, J. of Comput. Phys., 140, 459–480, https://doi.org/10.1006/jcph.1998.5901, 1998.

Smolarkiewicz P. K., and Szmelter, J. MPDATA: An edge-based unstructured-grid formulation, J. of Comput. Phys., 206, 624-649, https://doi.org/10.1016/j.jcp.2004.12.021, 2005.

Vieira, M. E. C., and Bordalo, A. A.: The Douro estuary (Portugal): a mesotidal salt wedge, Ocean. Acta, 23, 585-594, https://doi.org/10.1016/S0399-1784(00)01107-5, 2000.

Zarzuelo, C., López-Ruiz, A., Díez-Minguito, M., and Ortega-Sánchez, M.: Tidal and subtidal hydrodynamics and energetics in a constricted estuary, Estuar. Coast. Shelf Sci., 185, 55–68. https://doi.org/10.1016/j.ecss.2016.11.020, 2017.